Low temperature near-field scanning optical microscopy on infrared and terahertz photonic-crystal quantum cascade lasers

I. C. Moldovan-Doyen,[1,a)] G. Xu,[2] L. Greusard,[1] G. Sevin,[2] E. Strupiechonski,[2] G. Beaudoin,[3] I. Sagnes,[3] S. P. Khanna,[4] E. H. Linfield,[4] A. G. Davies,[4] R. Colombelli,[2] and Y. De Wilde[1,b)]

[1]*Institut Langevin, ESPCI ParisTech, CNRS, 10 rue Vauquelin 75231 Paris Cedex 05, France*
[2]*Institut d'Électronique Fondamentale, UMR 8622 CNRS, Université Paris–Sud, 91405 Orsay, France*
[3]*Laboratoire de Photonique et Nanostructures (LPN), CNRS, 91460 Marcoussis, France*
[4]*School of Electronic and Electrical Engineering, University of Leeds, Leeds LS2 9JT, United Kingdom*

(Received 31 January 2011; accepted 15 May 2011; published online 10 June 2011)

We report the development of a scattering-type near-field scanning optical microscope (sNSOM) which operates at temperatures down to 100 K with a scanning range of up to 400 μm. We have used this sNSOM to map the electromagnetic near-field on mid-IR and terahertz (THz) surface emitting quantum cascade lasers with photonic-crystal resonators. Mid-IR devices operate at $\lambda = 7.5$ μm (40 THz) while THz devices operate at $\lambda \approx 110$ μm (2.7 THz). The near-field images—in agreement with numerical calculations—demonstrate an instrument resolution of 100's nm.

[doi:10.1063/1.3597411]

Scattering-type near-field scanning optical microscopy (sNSOM) relies on the tip of an atomic force microscope to scatter an electromagnetic near-field into the far-field. Recording the scattered field while the tip is scanned on the sample surface produces an optical image with subwavelength resolution, and simultaneously the sample topography is recorded. sNSOM can be applied at any wavelength, unlike fiber-based NSOMs. Demonstrations target in fact the field distribution on mid-IR semiconductor lasers,[1] thermal and electrical surface plasmon sources,[2,3] and optical antennas.[4] Another application of sNSOMs at low photon energies, is the nanoscale observation of the dielectric contrast between materials,[5] or semiconductors and oxides.[6–8] To date sNSOMs are limited to room temperature (RT) operation. Aperture type probes operating down to liquid helium temperature have been reported, but their use is limited to visible and near-IR wavelengths.[9,10]

In this letter, we report the development of a low temperature sNSOM (LT-sNSOM) which operates at cryogenic temperatures down to 100 K. It features sub-λ resolution on an extremely wide frequency span, from the mid-IR to the terahertz (THz). We have used it to study the electromagnetic near-field at the surface of mid-IR and THZ quantum cascade lasers with photonic crystal (PhC) resonators. Note that for THz emitting devices, sNSOM operation at cryogenic temperatures is crucial and—to date—it has never been possible to characterize their emission in the near-field.

Among the main technical issues which had to be taken into account and solved to develop a LT-sNSOM are: (a) the collection optics which requires a high numerical aperture and good optical access to the tip located inside the cryostat chamber; (b) the thermal drift due to the thermal expansion/contraction of the tip and sample supports; and (c) the decrease in piezoelectric efficiency at low temperature.

The LT-sNSOM presented in Fig. 1 is mounted on an optical top supported by pneumatic vibration isolators. The scanning head fits inside the vacuum chamber of a home-built cryostat, made of a $15\times15\times15$ cm^3 hollow cube of aluminum connected with a Helitran®-LT3 continuous-flow cryogenic refrigeration system. Five facets are sealed. The sixth facet is closed by a square aluminum plate with a 40-mm-diameter central hole which allows one to insert the cold finger of the cryostat. Additional outlets are used for pumping and electrical connections. A turbo-molecular pump is used to reach a pressure $<10^{-5}$ mbar. The cold finger is a copper rod in contact with a heat exchanger, which is cooled with liquid nitrogen using the coaxial flow transfer line. The sample holder, also made of copper, is in thermal contact with the cryostat via a copper braid tightly screwed to them (Fig. 1). This provides a mechanically flexible and soft thermal connection which does not perturb the sample displacements during the scans, and it also prevents the propagation of mechanical vibrations. A glass epoxy thermal insulation is

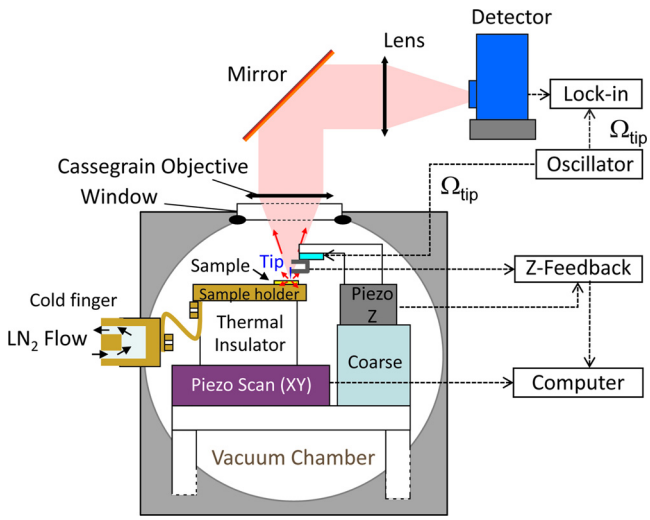

FIG. 1. (Color online) Schematic view of the LT-sNSOM.

a)Electronic mail: ioana.doyen@polytechnique.edu.
b)Electronic mail: yannick.dewilde@espci.fr.

inserted between the sample holder and the piezoelectric stage used to scan the sample laterally. The piezoelectric stage is fixed at the bottom of the cryostat chamber and it is therefore maintained at RT while the sample holder temperature can be set as low as 100 K. A maximum scan size of 400×400 μm^2 is achieved between 300 and 100 K. The cold finger temperature can be stabilized by a resistive heater connected to the temperature controller. The system is optimized so efficiently that the temperature can be stabilized within 10 mK during a scan of a few tens of minutes. As the linear thermal expansion coefficient typical for the materials used is approximately 10^{-5} K^{-1}, the thermal drift is limited to ~10 nm during a scan.

Our system uses a quartz tuning fork glued sideways on a piezoelectric disk made of lead zirconate titanate material used to excite its mechanical resonance. The tip of the LT-sNSOM is made from a short piece of tungsten wire, glued on one arm of the tuning fork.[11] The setup operates in intermittent contact mode with oscillation amplitude of ~100 nm and at a frequency $\Omega_{tip}\approx32$ kHz. The tip support is mounted on a piezoelectric scanner with a range of 16 μm, combined with a piezoelectric stepper motor which allows a coarse approach of the tip toward the sample surface. The scans and signal recordings are controlled using commercial electronics from RHK Technologies.

The collection optics and optical detector are located outside the cryostat chamber. The tip and sample are positioned a few millimeter under a small mid-IR or THz transparent window which is sealed to the upper facet of the cryostat chamber. The photons scattered by the tip at the sample surface propagate in free space through the cryostat window and they are collected by a Cassegrain objective (numerical aperture NA=0.5) mounted on a commercial microscope. The signal is detected with a nitrogen cooled mercury-cadmium-telluride detector (mid-IR detection), or with a helium cooled THz superconducting hot electron bolometer (THz detection). The detector output is connected to a lock-in amplifier.

To demonstrate the operation of the LT-sNSOM, we have recorded near-field images on PhC QC lasers operating at $\lambda=7.5$ μm (40 THz)[12,13] and 110 μm (2.7 THz).[14,15] Their PhC resonator is written on the top metallization, a gold layer which is the upper device electrode too. The mismatch between the modes supported by metalized and non-metalized regions yields the feedback for laser action.[16] We have chosen lasers whose surface emitted beam is doughnut-shaped, and whose divergence is 9° for mid-IR (Ref. 12) and 12° for THz devices.[14] Figure 2 shows microscope images and schematics of the devices, together with light-voltage-current characteristics measured at several temperatures.

The size of the mid-IR PhC QC laser is approximately 200×200 μm^2, and the hole radius of the metallic PhC is $r=0.52$ μm, with a lattice period $a=2.60$ μm. Figure 3 presents the results of the LT-sNSOM characterization. Figure 3(a) is a topographic image of an area of 20×20 μm^2 at the device top surface; Fig. 3(b) is the corresponding near-field image recorded simultaneously with a demodulation of the optical signal at Ω_{tip}. The images indicate that the field at the surface of the device is confined inside the holes of the photonic structure in good agreement with the numerical simulation of the monopole mode, as shown later in the text. Figure 3(c) present a near-field optical image acquired at 160 K, which demonstrates the capabilities of the LT-sNSOM for uses at various temperatures.

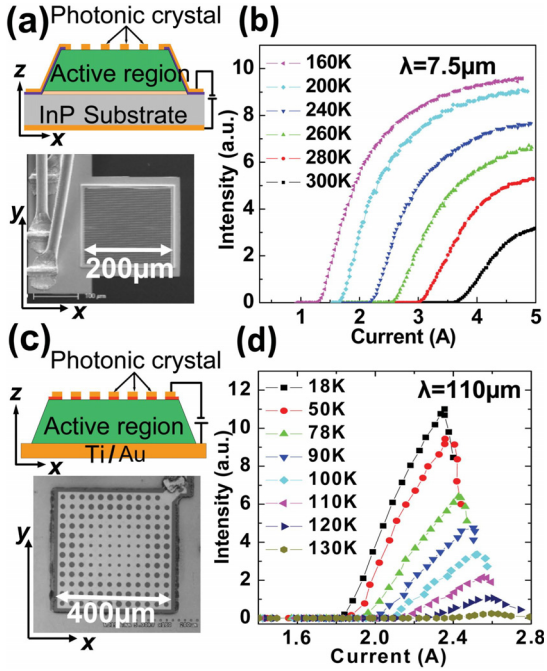

FIG. 2. (Color online) (a) Scanning electron microscopy (SEM) picture of a typical mid-IR PhC QC laser, and corresponding schematic device cross-section. The InP substrate is typically 200 μm-thick while the active-region is 3–4 μ-thick. (b) *L-I* curves measured in pulsed mode for the mid-IR PhC QC laser studied in this letter. The measurements at different heat-sink temperatures have been performed using 50 ns pulse widths at 84 kHz repetition rate. (c) SEM picture of a typical THz PhC QC laser, and corresponding schematic cross section. The PhC resonator is based on a square lattice design, and it comprises 12 photonic lattice periods. (d) *L-I* curves, at several heat-sink temperatures, measured in pulsed mode for the THz PhC QC laser studied in this letter. The measurements have been acquired using 333 ns pulse widths at a repetition rate of 33 kHz.

Figures 3(d) and 3(e) report the topographical image and the corresponding LT-sNSOM images of a 50×50 μm^2 re-

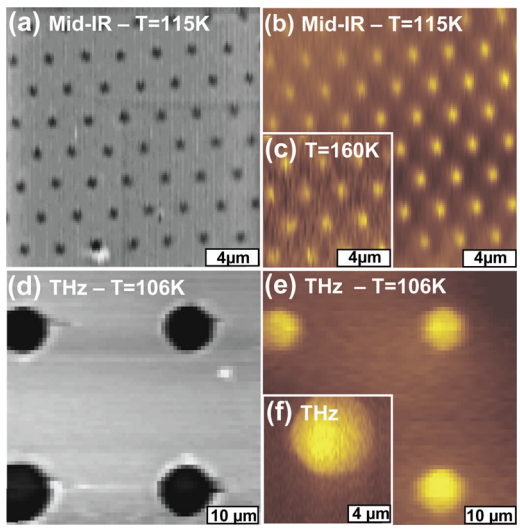

FIG. 3. (Color online) Images recorded at low temperature with the LT-sNSOM on a mid-IR and a THz PhC QC laser. (a) Topography image showing the PhC on the top electrode of a mid-IR PhC laser, and (b) corresponding near-field optical images recorded at 115 K. (c) Near-field optical image recorded at 160 K on the same device. (d) Topography image recorded near the center of the top electrode of a THz PhC laser, and (e) corresponding near-field optical image recorded at 106 K. (f) Near-field image at 106 K recorded around a hole of the THz PhC laser.

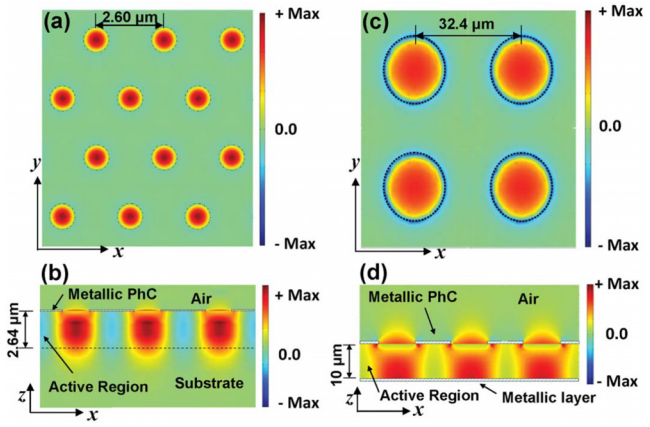

FIG. 4. (Color online) (a) Electric field component orthogonal to the layers (E_z) taken in a plane located 150 nm above the mid-IR device surface. The calculation is 3D and simulates an *infinitely periodic* structure. The dashed circles correspond to the edge of the air-holes in the top metallization. (Color online) (b) Distribution of E_z in the x-z section perpendicular to the PhC layer and across the centers of the air holes. [(c) and (d)] same calculations for the THz device.

gion at the top of a THz device operating at 106 K in pulse mode. The device size is approximately 400×400 μm^2 and the PhC lattice period is $a=32.4$ μm. The sNSOM measurements show that the field at the device surface is localized in the holes of the photonic structure. Figure 3(f) presents a LT-sNSOM image of a 15×15 μm^2 area of the device: the lateral resolution is estimated to a few hundreds of nanometer, which sets the resolution to better than $\lambda/100$. Note that, when measuring in the THz range, the LT-sNSOM images are obtained by demodulating the detector signal at the laser modulation frequency instead of Ω_{tip}. The intensity of the field scattered by the tip is proportional to the tip scattering cross section *times* the intensity of the near-field at the tip position, which contains both propagating and evanescent components. The scattering of the propagating components by the tip produces lateral intensity variations in the images on length scales of the order of the wavelength. On the other hand, the scattering of the evanescent components yields the subwavelength details in the images, as they are associated to the high spatial Fourier frequency components of the electromagnetic field.[17]

For both the mid-IR and THz PhC lasers investigated here, the lasing modes are the monopolar states at the Γ-point of the photonic band structure, which have the highest Q-factor. Monopolar modes exhibit energy maxima localized in the holes, in agreement with the sNSOM measurements in Fig. 3. However, the sNSOM measurement intrinsically probes the field slightly above the surface. The tip mainly scatters the electric field component oriented along its axis, E_z, which is orthogonal to the device surface. The signal at the detector results from the interference of the field scattered by the tip with the light produced by the laser which reaches the detector without being perturbed by the tip. Hence the small details observed in the sNSOM images are due to a subtle combination of linear and quadratic terms with E_z. Figures 4(a) and 4(c) report numerical simulations for the component of the electric field orthogonal to the surface (E_z) at a distance of 150 nm above the surface of the devices. Figures 4(b) and 4(d) show instead E_z in the *x-z* section perpendicular to the PhC plane and across the centers of the air holes. The electromagnetic field is calculated by solving the three-dimensional (3D) Helmholtz equation with Bloch boundary conditions using a finite elements approach.[18]

In conclusion, the operation of a low temperature (down to 100 K) sNSOM at mid-IR and THz frequencies has been demonstrated with extremely subwavelength resolutions. We have employed it to reveal the near-field electromagnetic distribution at the surface of PhC QC lasers. The results are in very good agreement with the theoretical analysis. The LT-sNSOM can find important applications for condensed matter studies. To date, there is indeed a lack of probes with nanoscopic resolution and able to operate at low temperature in this energy range. For instance, the LT-sNSOM could be used to obtain a nanoscopic vision of phase transitions such as metal/insulator or metal/superconductor transitions when used in transmission mode on thin film samples on a transparent substrate. Temperatures lower than 100 K should be achievable with the LT-sNSOM using liquid helium as cooling fluid.

We thank A. Babuty and S. Gresillon for useful support. We acknowledge financial support from the French National Research Agency (Grant Nos. ANR-07-NANO-039 "NanoFtir" and ANR-09-NANO-017 "Hi-Teq"), and from the *Triangle de la Physique* (RTRA "PhLARE"). The device fabrication has been performed at the nanocenter CTU-IEF-Minerve, partially funded by the "Conseil Général de l'Essonne."

[1]V. Moreau, M. Bahriz, R. Colombelli, P.-A. Lemoine, Y. De Wilde, L. R. Wilson, and A. B. Krysa, Appl. Phys. Lett. **90**, 201114 (2007).
[2]Y. De Wilde, F. Formanek, R. Carminati, B. Gralak, P.-A. Lemoine, K. Joulain, J.-P. Mulet, Y. Chen, and J.-J. Greffet, Nature (London) **444**, 740 (2006).
[3]A. Babuty, A. Bousseksou, J.-P. Tetienne, I. Moldovan Doyen, C. Sirtori, G. Beaudoin, I. Sagnes, Y. De Wilde, and R. Colombelli, Phys. Rev. Lett. **104**, 226806 (2010).
[4]N. Yu, E. Cubukcu, L. Diehl, M. A. Belkin, K. B. Crozier, F. Capasso, D. Bour, S. Corzine, and G. Höfler, Appl. Phys. Lett. **91**, 173113 (2007).
[5]B. Knoll and F. Keilmann, Nature (London) **399**, 134 (1999).
[6]A. J. Huber, F. Keilmann, J. Wittborn, J. Aizpurua, and R. Hillenbrand, Nano Lett. **8**, 3766 (2008).
[7]M. M. Qazilbash, M. Brehm, B.-G. Chae, P.-C. Ho, G. O. Andreev, B.-J. Kim, S. J. Yun, A. V. Balatsky, M. B. Maple, F. Keilmann, H.-T. Kim, and D. N. Basov, Science **318**, 1750 (2007).
[8]A. C. Jones, S. Berweger, J. Wei, D. Cobden, and M. B. Raschke, Nano Lett. **10**, 1574 (2010).
[9]R. D. Grober, T. D. Harris, J. K. Trautman, and E. Betzig, Rev. Sci. Instrum. **65**, 626 (1994).
[10]Y. Durand, J. C. Woehl, B. Viellerobe, W. Göhde, and M. Orrit, Rev. Sci. Instrum. **70**, 1318 (1999).
[11]Y. De Wilde, F. Formanek, and L. Aigouy, Rev. Sci. Instrum. **74**, 3889 (2003).
[12]G. Xu, V. Moreau, Y. Chassagneux, A. Bousseksou, R. Colombelli, G. Patriarche, G. Beaudoin, and I. Sagnes, Appl. Phys. Lett. **94**, 221101 (2009).
[13]G. Xu, Y. Chassagneux, R. Colombelli, G. Beaudoin, and I. Sagnes, Opt. Lett. **35**, 859 (2010).
[14]Y. Chassagneux, R. Colombelli, W. Maineult, S. Barbieri, S. P. Khanna, E. H. Linfield, and A. G. Davies, Appl. Phys. Lett. **96**, 031104 (2010).
[15]G. Sevin, D. Fowler, G. Xu, F. H. Julien, R. Colombelli, S. P. Khanna, E. H. Linfield, and A. G. Davies, Appl. Phys. Lett. **97**, 131101 (2010).
[16]M. Bahriz, O. Crisafulli, V. Moreau, R. Colombelli, and O. Painter, Opt. Express **15**, 5948 (2007).
[17]L. Novotny and B. Hecht, *Principle of Nano-Optics* (Cambridge, New York, 2006), p. 38.
[18]The commercial package COMSOL Multiphysics was employed.